THERMO-CHEMO-MECHANICAL MODEL FOR CONCRETE. I: HYDRATION AND AGING

By Miguel Cervera,[1] Javier Oliver,[2] and Tomás Prato[3]

ABSTRACT: In this work a coupled thermo-chemo-mechanical model for the behavior of concrete at early ages is proposed. The model allows simulation of the observed phenomena of hydration, aging, damage, and creep. It is formulated within an appropriate thermodynamic framework, from which the state equations are derived. In this first part, the formulation and assessment of the thermochemical aspects of the model are presented. It is based on the reactive porous media theory, and it can accurately predict the evolution in time of the hydration degree and the hydration heat production. The evolution of the compressive and tensile strengths and elastic moduli is related to the aging degree, a concept introduced to account for the effect of the curing temperature in the evolution of the mechanical properties. The short- and long-term mechanical behavior is modeled by means of a viscoelastic damage model that accounts for the aging effects. The formulation and assessment of the mechanical part of the model are relegated to a companion paper.

INTRODUCTION

Quality control during construction is one of the challenges of today's engineering practice, with regard to both the loss of durability and the functionality of the structures being built. In concrete technology, cracking is a cause of major concern, and it is primarily associated with thermal (and shrinkage) effects, particularly at early ages.

The chemical processes associated with the hardening of young concrete in the first days after casting are accompanied by significant temperature and volume changes. Initially, the reaction of hydration is highly exothermal, and the heat that is generated may produce increments of temperatures up to 50–60°C under adiabatic conditions. As the stiffness of concrete is then quite low, this usually leads to moderate, and mainly compressive, stresses. Later, when the stiffness has significantly increased, the concrete starts to cool down. The low conductivity of the material, differential effects due to the evolutive construction process, and convection phenomena with the environment may generate considerable thermal gradients. These, together with geometrical aspects and external restraints may develop relatively important tensile stresses. The tensile strength of the material is particularly small at this early age and cracking may appear. This may result in structural damage even before the structure is loaded and it may affect significantly the durability and serviceability of massive and reinforced concrete constructions.

To monitor this type of phenomena, a coupled thermo-chemo-mechanical model is needed to provide information on: the progress of the hydration process, the associated temperature rises, the evolution of the concrete strength and stiffness, as well as the development of tensile stresses and the possibility of cracking during the construction process.

This paper presents a thermo-chemo-mechanical model that considers many of the relevant features of the hydration and aging of concrete, in a format suitable for its implementation in the general framework of the finite-element method. First, a thermochemical model is proposed to model the evolution of the chemical reaction of concrete hydration and the heat that is generated during the process. The model is based on the theory of reactive porous media, within a consistent thermodynamic framework. The assumption of a closed chemical system allows a local description of the internal variables. Second, an aging model is proposed to describe the evolution of the mechanical properties of the material during the hydration process. To this end the concept of aging degree is introduced to monitor the evolution of the compressive strength. This allows accounting for the effect of the curing temperature in the final attained strength in a more realistic manner than the hydration degree or the maturity concepts. Other properties such as the tensile strength and the elastic moduli are then related to the compressive strength following usual engineering practice. Finally, different available experimental data sets are used to compare the observed behavior of conventional and high-performance concrete mixes at early ages with the simulations obtained using the proposed model.

HYDRATION MODEL

Hydration of concrete is a very complex process that involves quite a number of chemical and physical phenomena at the microscopic level. Basically, the free water present in the mixture reacts with the unhydrated cement to form hydrates. Portland cement is formed by four main mineral constituents: Calcium silicates such as C_3S and C_2S; calcium aluminates such as C_3A, and calcium aluminoferrites such as C_4AF. They react and combine with water to form different hydrates: Calcium silicate hydrate CSH, calcium hydroxide CH, ettringite Aft, monosulfate Afm, etc. The hydration mechanisms have been investigated for the last 100 years, but they are not clearly understood. However, it is clear that the rates of reaction of the individual constituents differ quite significantly. Therefore, the mathematical modeling of the interactions in a hydrating polymineral and polysize system is very complicated, as chemical, physical, stereological, and granular aspects must be considered. These complications make it mandatory to consider the phenomenon of clinker hydration rather than hydration of the individual compounds, and to state the problem in terms of the apparent, overall hydration process (van Breugel 1992b).

In view of this evidence, a macroscopic description of the hydration phenomenon is adopted for engineering purposes. From this point of view, hydration of concrete is a highly exothermic and thermally activated reaction, so that a thermochemical model is necessary for its modelization. State variables need to be defined and a proper thermodynamic frame-

[1]Asst. Prof. Struct. Anal., ETS Ingenieros de Caminos, 08034 Barcelona, Spain.
[2]Prof. Cont. Mech., ETS Ingenieros de Caminos, 08034 Barcelona, Spain.
[3]Grad. Res. Asst., ETS Ingenieros de Caminos, 08034 Barcelona, Spain.

Note. Associate Editor: Gilles Pijaudier-Cabot. Discussion open until February 1, 2000. Separate discussions should be submitted for the individual papers in this symposium. To extend the closing date one month, a written request must be filed with the ASCE Manager of Journals. The manuscript for this paper was submitted for review and possible publication on November 25, 1998. This paper is part of the ***Journal of Engineering Mechanics***, Vol. 125, No. 9, September, 1999. ©ASCE, ISSN 0733-9399/99/0009-1018–1027/$8.00 + $.50 per page. Paper No. 19717.

work must be provided to establish the relevant state equations.

The thermochemical model used in this work is based on the theory of reactive porous media developed by Coussy (1995), and its application to (chemoplastic) concrete as proposed by Ulm and Coussy (1995, 1996). Within this framework, the hydration process of concrete can be viewed, from a macroscopic level, as a chemical reaction in which the free water is a reactant phase that combines with the unhydrated cement to form combined water in the hydrates as a product phase. This implies that the (micro)diffusion of water through the layers of already formed hydrates can be considered as the dominant mechanism in the kinematics of the reaction.

Hydration Extent

Let us define the hydration (or reaction) extent χ as the number of moles of water combined per unit volume (related to the mass of water combined through the stoichiometric relationships and the molar masses). In the hypothesis of a closed chemical system, that is, without external supply or loss of water, the hydration extent can be considered as an internal variable of the system.

In these conditions, the free energy for the thermochemical system can be expressed in terms of one external variable—the temperature T, and one internal variable—the hydration extent

$$\Psi = \Psi(T, \chi) = V(T) + L(T, \chi) + H(\chi) \tag{1}$$

In this expression $V(T)$ = thermal contribution

$$V(T) = -\frac{1}{2}\frac{C}{T_0}(T - T_0)^2 \tag{2}$$

where T_0 = initial temperature; and C = heat capacity per unit volume (in a stress-free experiment), which can be assumed to be a constant material property, that is, independent of temperature and the hydration extent. The thermochemical coupling is represented by L, with the expression

$$L(T, \chi) = \frac{Q(\chi)}{T_0}(T - T_0) \tag{3}$$

where $Q(\chi)$ represents the amount of heat liberated per unit volume as a function of the reaction extent (in a stress-free and isothermal experiment). Most authors (Reinhardt et al. 1982; Rostassy et al. 1993; Torrenti et al. 1994; de Schutter and Taerwe 1995) identify the rate of heat liberation with the rate of hydration. This is equivalent to assuming a linear dependency of the form

$$Q(\chi) = Q_\chi \chi \tag{4}$$

where Q_χ = latent heat per unit of hydration extent, here assumed to be a constant material property.

Finally, $H(\chi)$ is the chemical contribution, which in this work will be taken as a cubic function, such as

$$H(\chi) = \frac{1}{3}k_\chi \chi^3 + \frac{1}{2}\left(\frac{A_{\chi 0}}{\chi_\infty} - k_\chi \chi_\infty\right)\chi^2 - A_{\chi 0}\chi \tag{5}$$

where k_χ and $A_{\chi 0}$ = material properties; and χ_∞ = final value of χ.

The state equations are obtained from (1) using Coleman's method as

$$S = -\partial_T \Psi(T, \chi) = \frac{1}{T_0}[C(T - T_0) - Q(\chi)] \tag{6}$$

$$A_\chi = -\partial_\chi \Psi(T, \chi) = k_\chi\left(\frac{A_{\chi 0}}{k_\chi \chi_\infty} + \chi\right)(\chi_\infty - \chi) - \partial_\chi L \tag{7}$$

where S = entropy; and A_χ = chemical affinity of the reaction, the thermodynamic forces conjugated to the temperature and the hydration extent, respectively. In the usual range of temperatures for concrete applications, the last term in (7), $-\partial_\chi L$, is considered negligible. Note that $A_{\chi 0}$ is the initial affinity of the reaction (at $\chi = 0$ and $T = T_0$), and that $A_\chi = 0$ for $\chi = \chi_\infty$ (at $T = T_0$). Note also that setting $k_\chi = 0$, a linear $A_\chi - \chi$ relationship is established (Ulm and Coussy 1995).

The chemical dissipation can then be expressed as

$$\mathcal{D}_{chem} = A_\chi \dot{\chi} \geq 0 \tag{8}$$

where $\dot{\chi}$, the time derivative of χ, is called the hydration rate. The model is completed with the evolution equation for the internal variable. The hydration rate is proportional to the chemical affinity, and it is usual to assume that the hydration reaction is thermoactivated. This leads to an Arrhenius-type equation such as

$$\dot{\chi} = \frac{A_\chi}{\eta_\chi}\exp\left(-\frac{E_a}{RT}\right) \tag{9}$$

where E_a = activation energy of the reaction; R = constant for ideal gases; and η_χ = viscosity due to microdiffusion of the free water through the already formed hydrates.

The ratio E_a/R can be experimentally determined, and it ranges from 3,000 to 8,000 K for concrete. Hansen and Nielsen (1985) and van Breugel (1992a) found that the apparent activation energy decreases with temperature, but it remains mostly constant above 20°C.

The viscosity η_χ is an increasing function of χ, because the growth of the layers of hydrates increases the diffusion time of the free water to reach the unhydrated cement. Inspired in de Schutter and Taerwe (1995), it is proposed to consider $\eta_\chi = \eta_\chi(\chi)$, so that

$$\eta_\chi = \eta_{\chi 0}\exp\left(\bar{\eta}\frac{\chi}{\chi_\infty}\right) \tag{10}$$

where $\eta_{\chi 0}$ and $\bar{\eta}$ = material constants. Note that the chemical dissipation can then be expressed as

$$\mathcal{D}_{chem} = \frac{A_\chi^2}{\eta_{\chi 0}}\exp\left(-\bar{\eta}\frac{\chi}{\chi_\infty}\right)\exp\left(\frac{-E_a}{RT}\right) \geq 0 \tag{11}$$

which is automatically satisfied if $\eta_{\chi 0} \geq 0$. Now, using (10), (9) may be written as

$$\dot{\chi} = \frac{k_\chi}{\eta_{\xi 0}}\left(\frac{A_{\chi 0}}{k_\chi \chi_\infty} + \chi\right)(\chi_\infty - \chi)\exp\left(-\bar{\eta}\frac{\chi}{\chi_\infty}\right)\exp\left(-\frac{E_a}{RT}\right) \geq 0 \tag{12}$$

where it can be seen that as χ increases and approaches its final value χ_∞, the reaction slows down and $\dot{\chi}$ tends to vanish.

Hydration Degree

For practical purposes, it is convenient to rewrite the model in terms of a normalized variable called hydration degree, defined as $\xi = \chi/\bar{\chi}_\infty$, where $\bar{\chi}_\infty$ is the final value of χ in ideal conditions, that is, with an adequate water/cement ratio to ensure full hydration and perfect contact between the water and the cement grains. In practice, these conditions are not fulfilled during curing and complete hydration of the concrete is not achieved, so $\chi_\infty < \bar{\chi}_\infty$, and therefore, $\xi_\infty < 1$ (Bentz et al. 1998). The final degree of hydration ξ_∞ is related to the water/cement ratio of the mixture (Byfors 1980; Waller et al. 1996), and it can be estimated as a function of it as, for instance (Pantazopoulo and Mills 1995)

$$\xi_\infty = \frac{1.031 w/c}{0.194 + w/c} \tag{13}$$

J. Eng. Mech., 1999, 125(9): 1018-1027

The hydration degree is not in conflict with the assumption of a closed chemical system. This assumption implies that the variation of the free water content in the mixture is equal to the variation of combined water in the solid hydrates. Therefore, in a closed chemical system, the hydration reaction will come to an end either when: (1) with an adequate initial free water content in the mix, there is no unhydrated cement left to react; or (2) with an insufficient initial free water content in the mix, all of the free water has already been consumed. In this second situation, which is very common in practice, the present definition of the hydration degree gives a realistic indication of the hydration degree of the mixture.

Now, defining the material constants $Q_\xi = Q_\chi \bar{\chi}_\infty$, $k_\xi = k_\chi \bar{\chi}_\infty^3$, $A_{\xi 0} = A_{\chi 0} \bar{\chi}_\infty$ and $\eta_{\xi 0} = \eta_{\chi 0} \bar{\chi}_\infty^2$, we can write the thermochemical coupling term in (3) as

$$L(T, \xi) = \frac{Q(\xi)}{T_0}(T - T_0) \tag{14}$$

where $Q(\xi) = Q_\xi \xi$ because of the linear assumption in (4). Note that because of this, the hydration degree can also be defined as $\xi = Q/Q_\infty$, where Q_∞ is the final amount of liberated heat in ideal conditions (Torrenti 1992; de Schutter and Taerwe 1995; Boumiz et al. 1996; Acker 1997).

The chemical term in (5) can now be rewritten as

$$H(\xi) = \frac{1}{3} k_\xi \xi^3 + \frac{1}{2}\left(\frac{A_{\xi 0}}{\xi_\infty} - k_\xi \xi_\infty\right)\xi^2 - A_{\xi 0}\xi \tag{15}$$

The evolution of the newly defined internal variable now reads

$$\dot{\xi} = \frac{k_\xi}{\eta_{\xi 0}}\left(\frac{A_{\xi 0}}{k_\xi \xi_\infty} + \xi\right)(\xi_\infty - \xi)\exp\left(-\bar{\eta}\frac{\xi}{\xi_\infty}\right)\exp\left(-\frac{E_a}{RT}\right)$$
$$= \tilde{A}_\xi(\xi)\exp\left(-\frac{E_a}{RT}\right) \geq 0 \tag{16}$$

The function $\tilde{A}_\xi(\xi) = A_\xi/\eta_\xi$ was introduced in Ulm and Coussy (1996) as a normalized affinity that completely characterizes the macroscopic hydration kinetics for a given concrete mixture. This function can be obtained experimentally from an adiabatic calorimetric test, as explained below. The model presented here proposes an analytical expression for this function.

Thermal Field Equation

From the first and second principles of thermodynamics, the thermal field equation can be written, in its entropy rate form, as

$$T_0 \dot{S} = R_{ext} - \nabla \cdot \mathbf{Q} + \mathcal{D} \tag{17}$$

where R_{ext} = external volume heat sources; $\mathbf{Q}$ = heat flux; and $\mathcal{D}$ = dissipation (here, $\mathcal{D} = \mathcal{D}_{chem}$), which is usually considered negligible compared with the other terms in the equation. Taking the time derivative of the state equation for the entropy [(6)], yield $T_0\dot{S} = C\dot{T} - \dot{Q} = C\dot{T} - Q_\xi\dot{\xi}$, so that the thermal field equation can be written in its usual temperate rate form, as

$$C\dot{T} - Q_\xi\dot{\xi} = R_{ext} + k_T \nabla \cdot (\nabla T) \tag{18}$$

where Fourier's law has been used ($\mathbf{Q} = k_T \nabla T$), with k_T being the thermal conductivity. Note that the term due to the hydration heat $\dot{Q}$ actually acts as a nonlinear internal heat source. The thermochemical model described explicitly allows the determination of this term through (16).

Experimental Determination

During the performance of an adiabatic calorimetric test, the thermal field equation [(18)] reduces to

$$C\dot{T}^{ad} = Q_\xi \dot{\xi} \tag{19}$$

This, together with the linear relationship $Q(\xi) = Q_\xi \xi$, allows relating the hydration degree to the temperature rise in the adiabatic experiment in the form

$$\frac{\xi}{\xi_\infty} = \frac{T^{ad}}{T_\infty^{ad} - T_0} \tag{20}$$

where T_0 = initial temperature; T^{ad} = measured temperature of concrete along the experiment; and T_∞^{ad} = final reached temperature. Also, the average value of the constant Q_ξ for the experiment can be evaluated as

$$Q_\xi = \frac{C}{\xi_\infty}(T_\infty^{ad} - T_0) = C(\bar{T}_\infty^{ad} - T_0) \tag{21}$$

where $\bar{T}_\infty^{ad}$ = final reached temperature in ideal conditions (when $\xi_\infty = 1$). Now, using (16), (19), and (21), the normalized affinity can be expressed as

$$\tilde{A}_\xi(\xi) = \frac{\xi_\infty \dot{T}^{ad}}{T_\infty^{ad} - T_0}\exp\left(\frac{E_a}{RT^{ad}}\right) \tag{22}$$

where $\dot{T}^{ad}$ = measured temperature rate along the experiment. Therefore, it is possible to measure the relationship $\tilde{A}_\xi - \xi$ experimentally. The use of the analytical expression proposed in the present model for this function [(16)], allows the definition of the experimentally obtained function by the calibration of three material properties, $k_\xi/\eta_{\xi 0}$, $A_{\xi 0}/k_\xi$, and $\bar{\eta}$, which fully characterize the chemical behavior of the concrete mix.

Fig. 1(a) shows the temperature rise versus time in an adiabatic test for a conventional concrete as computed from the model and compared with experimental results. The hydration reaction starts quite slowly, because of the low initial chemical affinity. However, it accelerates after the so-called activation period. Afterward, the reaction is very fast in adiabatic conditions, due to its thermoactivated character. Temperature rises rapidly during the first hours, until the hydration degree reaches a value close to the percolation threshold. An inflexion is then evident in the curve, and the reaction slows down significantly. Fig. 1(b) corresponds to the graphical representation of the normalized chemical affinity introduced in (16). The maximum in the hydration rate corresponds to the inflexion point in the temperature rise. Figs. 1(c) and 1(d) show the corresponding curves for a high-performance concrete with addition of silica fume.

Hydration Degree and Maturity

Since its introduction by Saul (1951), many aging models for concrete are defined in terms of maturity or equivalent age, which is an empirical concept introduced to account for the influence of temperature during the curing process (Rastrup 1954; Plowman 1956; Oloukon et al. 1990). Although many expressions have been proposed for the evolution of maturity, it is generally accepted that hydration of concrete is governed by an Arrhenius-type equation (Copeland et al. 1960; Carino 1981; Hansen and Nielsen 1985; Chengju 1989), which leads to a maturity concept defined as

$$\mu_t(T, t) = \int_0^t \exp\left[-\frac{E_a}{R}\left(\frac{1}{T(\tau)} - \frac{1}{T_{ref}}\right)\right] d\tau \tag{23}$$

where t = time, or in rate form, as

$$\dot{\mu}_t = \exp\left[-\frac{E_a}{R}\left(\frac{1}{T(t)} - \frac{1}{T_{ref}}\right)\right] \tag{24}$$

where T_{ref} = reference temperature for which maturity coincides with real time. From a more fundamental standpoint, it is clear that the concept of maturity must be related to the

J. Eng. Mech., 1999, 125(9): 1018-1027

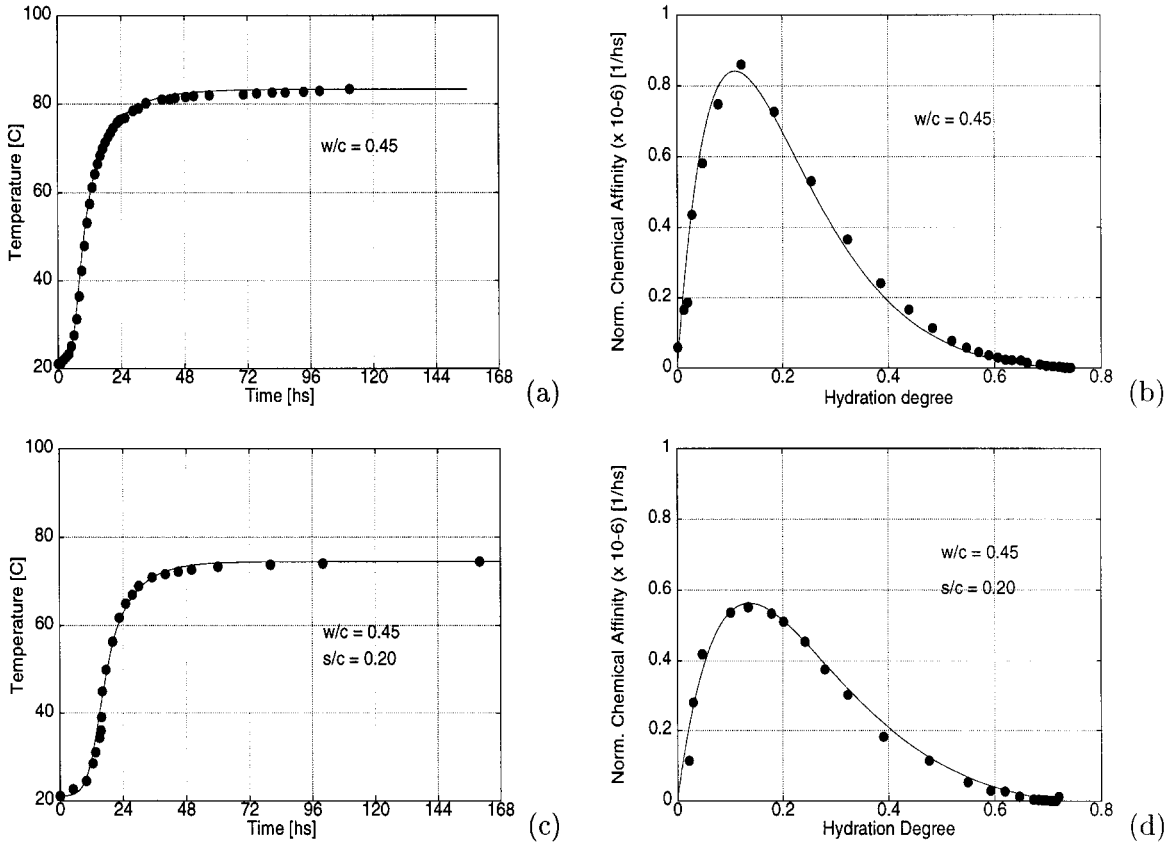

FIG. 1. Temperature Evolution and Normalized Affinity for Adiabatic Tests

concepts of hydration extent and degree. In the present model, comparing (16) and (24) yields the relation (Ulm and Coussy 1996)

$$\frac{d\xi}{d\mu_t} = \exp\left(-\frac{E_a}{RT_{ref}}\right)\tilde{A}_\xi(\xi) = c_{ref}\tilde{A}_\xi(\xi) \tag{25}$$

where c_{ref} = constant. This differential equation can be integrated to obtain the relation between maturity and hydration degree for a given curing process. This means that, in general, either of the two variables can be used indistinctly for the definition of the aging models, although the hydration degree concept provides a link with a consistent thermodynamic framework that it is lacking in the concept of maturity. However, neither the hydration degree by itself, nor, alternatively, the concept of maturity can determine uniquely the development of strength for a given temperature. This is due to the significant role that temperature has in the development of strength at early ages. This will be discussed in the next section.

AGING MODEL

The change in the relative proportions and physical properties of the basic constituents of concrete during the chemical reaction of hydration is a phenomenon known as aging. From a macroscopic level, aging is observed as the change in the mechanical properties of the mortar as a function of the hydration degree. The influence of the hydration process is qualitatively the same for mortar and concrete (Neville 1981) and the relation between their strength (for the same *w/c* ratio) is linear (Walker and Bloem 1958).

From a microscopic level the hydration of cement consists of the following (Acker 1988):

1. An initial suspension phase during the first 1–2 h after the addition of water to the cement, in which gel starts to form around the grains but no forces exist between the particles.
2. An intermediate setting phase during the 3–24 h after the mixing, which corresponds to the formation of outer products outside the grains and inner products inside them, and the development of the basic solid skeleton between the grains.
3. A final hardening phase, between 1 and 28 days after the mixing, which corresponds to the formation of the stable solid skeleton by the filling of the capillary and interstitial pores by the hydrates. Furthermore, when considering the aging of concrete, the microstructural behavior of the interphase between the cement matrix and the aggregates must also be taken into account.

During past decades, many aging models have been proposed in which the mechanical properties of young concrete were expressed in terms of the hydration degree, or alternatively, of the maturity (Rastrup 1954; Plowman 1956; Oloukon et al. 1990). The basic assumption for these models is that concretes of the same mix at the same hydration degree (or maturity) have the same strength, independent of the hydration kinetics occurring to reach that hydration degree (or maturity).

However, there is experimental evidence that the evolution of the concrete strength depends not only on the degree of hydration, but also on the kinetics of the hydration reaction (Byfors 1980; Volz et al. 1981; Carino 1981; Chengju 1989; Shi and Day 1993; Bland et al. 1994; Wild et al. 1995; Tan and Gjorv 1996; Kim et al. 1998). For instance, Verbeck and Helmuth (1968) found that the strength of companion mortar specimens hydrated at 50°C was about 20% lower than that of specimens hydrated at 5°C, at a given degree of hydration.

These results are consistent with electronic microscope observations that show that the increase of the curing temperature produces changes in the density and distribution of cement grains. This phenomenon is more pronounced when the tem-

J. Eng. Mech., 1999, 125(9): 1018-1027

perature rise occurs earlier in the setting and hydration process (Kjellsen and Detwiler 1993). Because the hydration of cement is a thermoactivated reaction, at low curing temperatures the hydration products form slowly and the free water can diffuse through the forming solid skeleton and the hydrates deposit uniformly. On the other hand, curing at high temperatures increases the rate of hydration. The hydration products form faster and they deposit close to the unhydrated cement grains. The microdiffusion process of the free water through the forming solid skeleton is hindered and the void interstitial pores are left (Verbeck and Helmuth 1968). In Kjellsen (1990), the formation of a shell around the cement grains as a result of the higher rate of hydration can be observed. The strength of mortar is influenced by the uniformity of the microstructure, and the mechanical properties depend on the size and distribution of the interstitial pores between the grains and the cement paste. Low curing temperatures lead to a uniform distribution of hydration products and interstitial pores. On the contrary, at high curing temperatures the solid skeleton is stronger and more dense, but the pores left during the hydration process are larger. In these conditions, the mechanical properties of the resulting microstructure, such as the strength and the elastic modulus, are significantly reduced.

In view of this, it is concluded that concrete strength cannot be related directly to the hydration degree (or maturity), and therefore, the mechanical properties cannot be obtained without the consideration of the hydration kinetics. A realistic aging model must be established in which the mechanical properties act as internal-like variables, and their evolution laws must at least be formulated in terms of hydration degree and temperature.

The aging model presented here contemplates the evolution of the compressive and tensile uniaxial strengths and the uniaxial elastic modulus during the hydration process of the concrete, because these are the basic parameters used in the mechanical damage model described in the companion paper. For simplicity, Poisson's ratio is assumed to remain constant. The effect of the curing temperature is explicitly included in the model.

Compressive Strength

The parameter mainly used in practice for the mechanical characterization of concrete is the compressive strength f^-. Other relevant mechanical properties such as the tensile strength f^+ and the elastic modulus E are usually estimated as functions of f^-. This is certainly the common rule in most codes of practice (*ACI* 1987; *CEB-FIP* 1990; *Instrucción* 1991). Here, the same procedure will be followed.

It is common practice for aging models to consider the evolution of the compressive strength of concrete as a direct function of the hydration degree, defining an aging function $\lambda_f^-(\xi)$, in the form

$$f^-(\xi) = \lambda_f^-(\xi) f_\infty^- \tag{26}$$

where f_∞^- = final compressive strength and the aging function satisfies the conditions $\lambda_f^-(\xi) \geq 0$ and $\lambda_f^-(0) = 0$, $\lambda_f^-(\xi_\infty) = 1$. This expression, independent from temperature, can be considered valid for isothermal curing conditions at a given reference temperature T_{ref}. Linear, bilinear, parabolic, and cubic expressions have been proposed in the literature for the aging function (Byfors 1980; Neville 1981; Parrot et al. 1990; Torrenti 1992; Rostassy et al. 1993; de Schutter and Taerwe 1995; Mak and Torri 1995; Ulm and Coussy 1995). In rate form, this relation can be written as

$$\dot{f}^-(\xi) = \dot{\lambda}_f^-(\xi) f_\infty^- = \lambda_{f,\xi}^- \dot{\xi} f_\infty^- \tag{27}$$

where $\lambda_{f,\xi}^- = d\lambda_f^-/d\xi$ represents the relation between the hydration rate and the hardening rate. In this work it will be assumed that $\lambda_f(\xi)$ is a parabolic function of ξ, and therefore, the derivative $\lambda_{f,\xi}^-$ can be written as

$$\lambda_{f,\xi}^-(\xi) = A_f \xi + B_f \quad \text{for} \quad \xi \geq \xi_{set} \tag{28}$$

where ξ_{set} = value defining the end of the setting phase, just when the concrete may begin to be considered a solid (Byfors 1980; Boumiz et al. 1996; Acker 1997). Values $\xi_{set} = 0.1-0.4$ have been proposed in the literature, depending on the type of cement and the water/cement ratio (Torrenti 1992; de Schutter and Taerwe 1996). A linear relationship with $A_f = 2 f_{set}^-/(f_\infty^- \xi_{set}^2)$ and $B_f = 0$ may be considered for $\xi \leq \xi_{set}$.

However, as explained above, the effect of the curing temperature on the evolution of the compressive strength makes it necessary to relate this evolution to the hydration kinetics. To this end, let us introduce an aging internal variable κ, so that (26) is replaced by

$$f^-(\kappa) = \kappa f_\infty^-, \quad \kappa \geq 0 \tag{29}$$

Note that κ can be considered a normalized strength variable. Thus, it will be called an aging degree. It will be shown in the companion paper that the aging degree controls the evolution of the chemical hardening.

The evolution of the aging degree must be related to the hydration kinetics and the temperature. Inspired in (27), it is proposed to take

$$\dot{\kappa} = \lambda_T(T)\lambda_{f,\xi}^-(\xi)\dot{\xi} \geq 0 \tag{30}$$

where the term λ_T has been included to explicitly account for the influence of the curing temperature. For the term λ_T, we propose the expression

$$\lambda_T = \left(\frac{T_T - T}{T_T - T_{ref}}\right)^{n_T} \tag{31}$$

where T_{ref} = reference temperature for the determination of f_∞^-; T_T represents the maximum temperature at which hardening of concrete may occur; and n_T = a material property. Note that for $T > T_{ref}$, $\lambda_T \leq 1$ results, thus diminishing the increase of strength; on the contrary, for $T \leq T_{ref}$, $\lambda_T \geq 1$ results, thus enhancing the increase of strength.

Substituting (16) into (30), we have

$$\dot{\kappa} = \lambda_T(T)\lambda_{f,\xi}^-(\xi)\tilde{A}_\xi(\xi)\exp\left(-\frac{E_a}{RT}\right) \tag{32}$$

which clearly expresses the dependency of the aging variable both on the hydration degree and on temperature.

Fig. 2(a) shows the evolution time of the hydration degree for a mixture cured in isothermal conditions at three different temperatures (5°C, T_{ref} = 20°C and 40°C). Note that due to the thermoactivated character of the hydration reaction, the rate of hydration is faster at higher temperatures. Nevertheless, the final degree of hydration is the same in all cases, as it depends basically on the initial water content of the mixture. Fig. 2(b) shows the evolution in time of the compressive strength (and therefore, the aging degree) for the same mixture cured at those same temperatures. As in Fig. 2(a), the rate of hardening is faster at higher temperatures; however, the final attained strength is smaller at higher curing temperatures. This effect of the curing temperature cannot be reproduced by aging models based exclusively on the hydration degree, or, alternatively, on the concept of maturity or equivalent age. On the contrary, the present model reproduces this effect appropriately.

It should be noted that the present approach corresponds to the physical observation that two concrete samples with identical mixing, but cured at different temperatures, show different strengths for the same hydration degree. In Kjellsen and

J. Eng. Mech., 1999, 125(9): 1018-1027

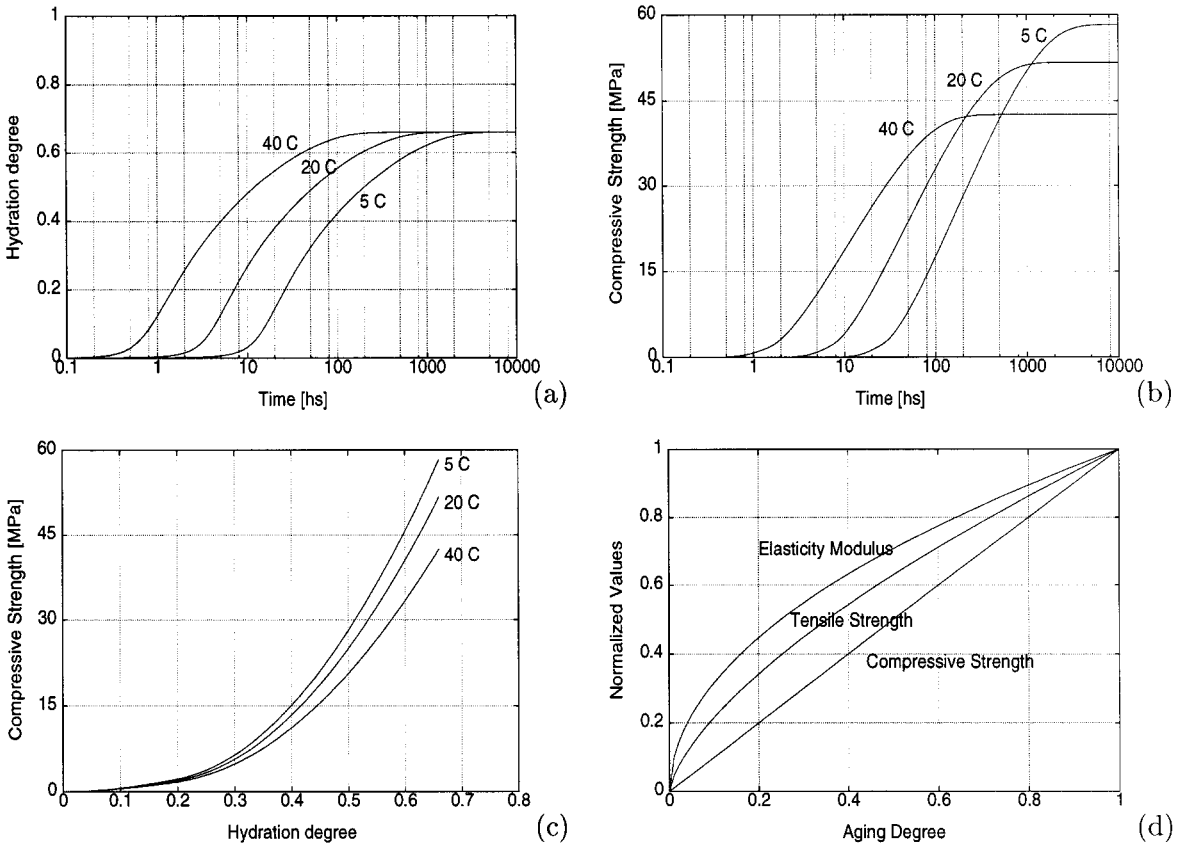

FIG. 2. (a) Evolution of Hydration Degree at Different Curing Temperatures; (b) Evolution of Compressive Strength at Different Curing Temperatures; (c) Strength versus Hydration Degree at Different Curing Temperatures; (d) Relative Mechanical Aging

Detwiler (1993), the activation energy of the reaction was considered a function of the temperature and the hydration degree to introduce what they called the effect of ''retardation'' due to high curing temperature. Even if good matches are obtained in terms of curves showing strength increase versus time, this alternative approach is incorrect from the physical standpoint, as this will not only affect the evolution of strength but also the hydration kinetics in an unrealistic manner.

Experimental Determination

The evolution of the hydration degree can be related to the evolution of the hydration degree [see (30)], in the form

$$\frac{d\kappa}{d\xi} = \lambda_T(T)\lambda_{f,\bar{\xi}}^{-}(\xi) \tag{33}$$

which shows that, for a given hydration degree $\bar{\xi}$, the relation between the compressive strength for two identical mixtures cured in isothermal conditions at two different temperatures T_1^{iso} and T_2^{iso}, is

$$\frac{\kappa_1^{iso}(\bar{\xi})}{\kappa_1^{iso}(\bar{\xi})} = \frac{\lambda_T(T_1^{iso})}{\lambda_T(T_2^{iso})} = \left(\frac{T_T - T_1^{iso}}{T_T - T_2^{iso}}\right)^{n_T} \tag{34}$$

This is graphically indicated in Fig. 2(c), which shows the evolution of strength versus hydration degree under different curing temperatures.

In particular, for $\bar{\xi} = \xi_\infty$ and $T_2^{iso} = T_{ref}$, and considering that, at reference temperature, $\lambda_T(T_{ref}) = 1$, and therefore, $\kappa_\infty^{ref} = 1$, this yields

$$\kappa_\infty^{iso} = \lambda_T(T^{iso}) = \left(\frac{T_T - T^{iso}}{T_T - T_{ref}}\right)^{n_T} \tag{35}$$

This means that the final compressive strength attained in isothermal conditions, according to (29), $f^{-}(\kappa_\infty^{iso}) = \kappa_\infty^{iso} f_\infty^{-}$, where $f^{-}(\kappa_\infty^{iso})$ will be greater or lesser than the reference strength f_∞^{-}, depending on T^{iso} being lesser or greater than T_{ref}, respectively.

Consequently, it is enough to measure the final compressive strength in an isothermal test carried out at a temperature that is different from the reference one to be able to determine the exponent n_T.

The experimental determination of the function $\lambda_{f,\bar{\xi}}^{-}(\xi)$, or the constants A_f and B_f if the expression in (28) is adopted, requires the experimental determination of the hydration degree. This can be easily done in an adiabatic test as explained above [see (20)].

Tensile Strength and Elastic Moduli

The final tensile strength is usually considered to be related to the final compressive strength. For this relation most codes of practice (*ACI* 1987; *CEB-FIP* 1990; *Instrucción* 1991) recommend the expression $f_\infty^{+} = A_+(f_\infty^{-})^{2/3}$, where A_+ is a constant. If this relationship holds for the whole aging process, and considering (29), it follows that (Rostassy et al. 1993)

$$f^{+}(\kappa) = \lambda_f^{+}(\kappa) f_\infty^{+} = \kappa^{2/3} f_\infty^{+} \tag{36}$$

The final elastic modulus is also often considered a function of the final compressive strength (*CEB-FIP* 1990; *Instrucción* 1991), a usual dependency being of the form $E_\infty = A_E(f_\infty^{-})^{1/2}$, where A_E is a constant. If this dependency holds for the whole aging process, and considering (29), we can write

$$E(\kappa) = \lambda_E(\kappa) E_\infty = \kappa^{1/2} E_\infty \tag{37}$$

With the above relationships and the hypothesis of constant Poisson's ratio, the bulk and shear moduli can be written as

$$K(\kappa) = \lambda_E(\kappa) K_\infty; \quad G(\kappa) = \lambda_E(\kappa) G_\infty \tag{38a,b}$$

J. Eng. Mech., 1999, 125(9): 1018-1027

with the usual expressions $K_\infty = E_\infty/3(1 - 2\nu)$ and $G_\infty = E_\infty/2(1 + \nu)$.

Fig. 2(d) shows curves of relative evolution of the normalized compressive strength, tensile strength, and elastic modulus in terms of the aging degree. The functional dependencies expressed by (36) and (37) need to be experimentally confirmed. In de Schutter and Taerwe (1996) it was reported that the tensile strength develops faster than the compressive strength, but slower than the elastic modulus. In de Schutter and Taerwe (1997), three-point bending tests were performed on unnotched prisms at different concrete ages, ranging from 24 to 28 days, to study the evolution of the softening behavior during hardening. The experimentally found exponent for the tensile strength varied between 0.46 and 0.88, with an average value of 0.70. These results are consistent with the present proposal of a 2/3 exponent.

Tensile and Compressive Fracture Energies

The stored elastic energy per unit volume is proportional to the square of the stress and inversally proportional to the elastic moduli of the material. The energies released per unit area when damage or fracture (under tension or compression) occurs are considered material properties called the tensile and compressive fracture energies G_f^+ and G_f^-, respectively. These material properties increase as the hydration of concrete progresses, and therefore, they depend on the aging degree

$$G_f^+(\kappa) = \lambda_G^+(\kappa) G_{f\infty}^+; \quad G_f^-(\kappa) = \lambda_G^-(\kappa) G_{f\infty}^- \qquad (39a,b)$$

Here, we will assume that the fracture energies are proportional to the maximum stored elastic energy per unit volume, thus establishing the dependence of the fracture energies on the aging degree as

$$\lambda_G^+(\kappa) = \frac{\lambda_f^+(\kappa)^2}{\lambda_E(\kappa)} = \kappa^{5/6} \qquad (40)$$

$$\lambda_G^-(\kappa) = \frac{\lambda_f^-(\kappa)^2}{\lambda_E(\kappa)} = \kappa^{3/2} \qquad (41)$$

These functional dependencies also need to be experimentally confirmed. The experimentally found exponent for the tensile fracture energy in de Schutter and Taerwe (1997) varied between 0.46 and 1.10, with an average value of 0.87. These results are consistent with the present proposal of a 5/6 exponent.

NUMERICAL SIMULATIONS

This section presents an assessment of the thermochemical model described above. All of the problems presented are solved advancing step-by-step in time. For each time step, the thermal equation [(18)] is solved, together with the differential equation governing the chemical process [(16)].

Hydration Model

This subsection compares available experimental data with numerical predictions obtained using the thermochemical model that is proposed above. Therefore, all of the tests in this subsection were conducted in adiabatic conditions.

Bentz et al. (1998) conducted a series of experimental adiabatic tests to measure the temperature rise observed during the curing of conventional and high-performance concretes. We have selected results reported for conventional concrete w/c = 0.45, as well as for high-performance concrete with w/c = 0.45 and silica fume-to-cement mass ratio s/c = 0.20. The material properties used for the numerical simulation are listed in Table 1. Note that only the chemical related properties are necessary. The values used for the final degree of hydration ξ_∞ are those given by (13).

TABLE 1. Material Properties for Numerical Simulations

Properties (1)	Bentz (I) (2)	Bentz (II) (3)	Kjellsen (4)	Wild et al. (5)
w/c	0.45	0.45	0.50	0.50
s/c	0.00	0.20	0.00	0.00
C (10^6 J/m^3 °C)	2.33	2.33	2.07	2.07
k_T (10^3 J/m h °C)	5.40	5.40	5.40	5.40
T_0 (°C)	21.0	21.0	21.0	21.0
ξ_∞	0.72	0.72	0.75	0.75
$k_\xi/\eta_{\xi 0}$ (10^8 1/h)	0.28	0.15	0.32	0.20
$\bar{\eta}$	5.30	4.00	6.50	6.00
$A_{\xi 0}/k_\xi$ (10^{-5})	0.50	0.50	1.00	1.00
E_a/R (10^3 K)	5.00	5.00	5.00	3.00
Q_ξ (10^8 J/m^3)	2.02	1.73	1.25	1.25
ξ_{set}	—	—	0.20	0.20
A_f	—	—	0.47	0.87
B_f	—	—	0.66	0.15
f_∞^- (MPa)	—	—	58.0	88.0
T_{ref} (°C)	—	—	20.0	20.0
T_T (°C)	—	—	100.0	100.0
n_T	—	—	0.40	0.25

Fig. 1 shows the comparison between the experiments and the results obtained using the proposed thermochemical model. The dots represent the experimental values; the solid line represents the prediction by the model.

Fig. 1(a) shows the temperature rise versus time for the conventional concrete mix. The hydration reaction starts quite slowly, because of its very low initial chemical affinity. However, it accelerates after the first 2–3 h, the so-called activation period. Afterward, the reaction is very fast in adiabatic conditions, due to its thermoactivated character. Temperature rises rapidly during the first 12 h, until the hydration degree reaches a value close to ξ_{set} = 0.2, which can be considered the percolation threshold. An inflexion is then evident in the curves, and the reaction slows down significantly. The process is nearly completed after 5 days. Note that the overall behavior is very well captured, and that the deviations between the model predictions and the experimental measurements are minimal. Fig. 1(b) shows a graphical representation of the normalized chemical affinity introduced in (16). The experimental values have been obtained from the corresponding temperature versus time measured curves using the procedure described by (22). The above-described stages during the hydration process are also quite evident in this figure. The maximum in the hydration rate corresponds to the inflexion point in the temperature rise.

Figs. 1(c) and 1(d) show results corresponding to the high-performance concrete with silica fume addition. Note that the proposed model is also able to match the experimental behavior of this type of concrete mix. This means that the pozzolanic reaction between calcium hydroxide (CH) and silica fume (S) does not differ too much from the other chemical reactions that take place during the hydration of conventional portland cement concretes. This is a fortunate and useful verification of the possibilities of the model. However, this does not mean that the present model can be used for other types of concrete mixes without careful consideration. For instance, the experimental evidence shows that concrete made with blast furnace slag cement exhibits a different heat production rate than that of conventional portland cement (de Schutter and Taerwe 1995). These specific features are not contemplated in the present model.

Aging Model

This subsection compares available experimental data with numerical predictions obtained using the aging model that is

J. Eng. Mech., 1999, 125(9): 1018-1027

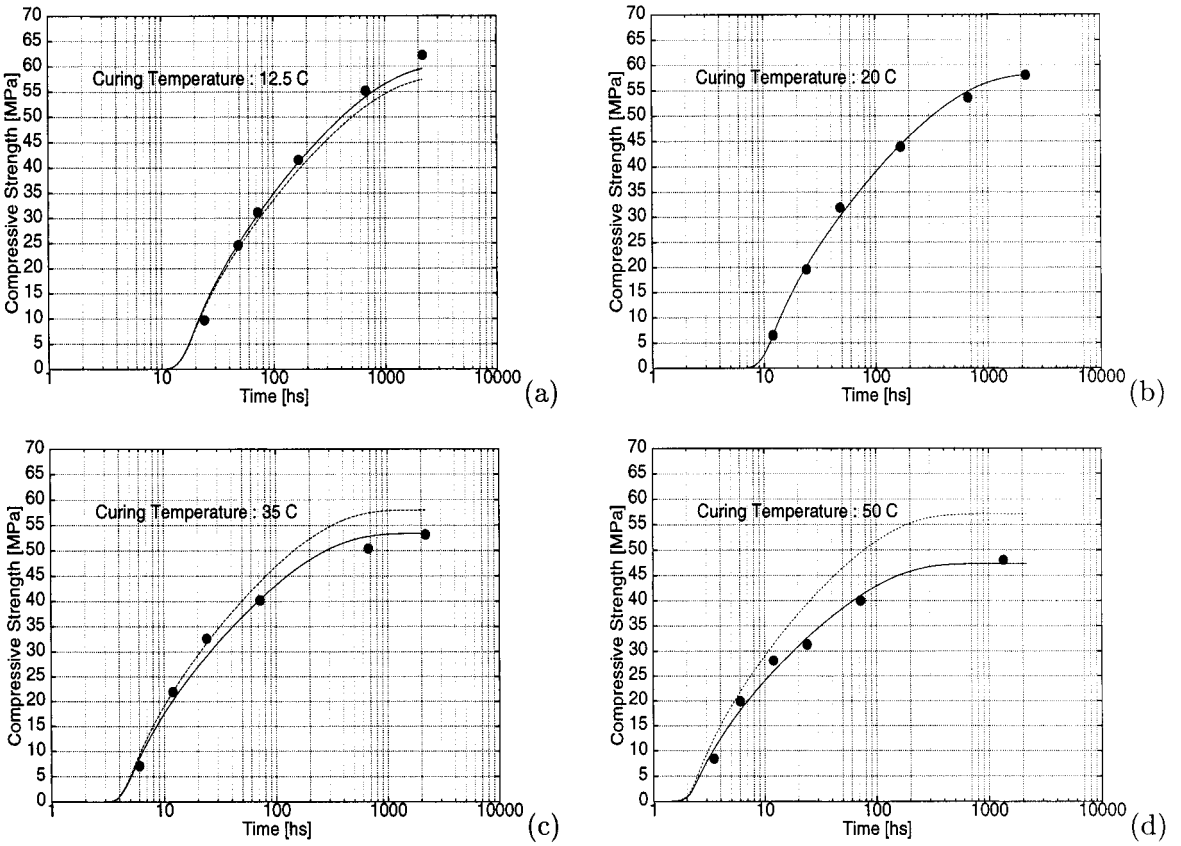

FIG. 3. Strength Evolution for Kjellsen's Tests

proposed above. The experimental sets focused on the influence of the curing temperature in the evolution of the compressive strength. Therefore, all of the tests in this subsection were conducted in isothermal conditions.

Kjellsen's Tests

The first experimental set consists of tests conducted by Kjellsen (1990), and they are also reported in Kjellsen and Detwiler (1993). They refer to $w/c = 0.5$ mortar, the cement used being ASTM Type I/III. The material properties used for the numerical simulation are listed in Table 1. Note that only the chemical and aging related properties are necessary. The value used for the final degree of hydration ξ_∞ is estimated using (13).

Fig. 3 shows the compressive strength versus time curves obtained for the curing temperatures T_0 = 12.5, 20, 35, and 50°C, respectively. The dots represent the experimental values, the solid line is the prediction by the model, and the dashed line is the result obtained when neglecting the influence of the temperature in the evolution of the aging function, that is, taking $\lambda_T = 1$ in (30).

The effect of the curing temperature is twofold: (1) The thermoactivated character of the hydration reaction is very evident in these plots, as the process of hardening is accelerated by the increase in curing temperature; and (2) the significant loss of strength with increasing curing temperature is clear. The first effect is particularly evident at the initiation of the hydration process, with an activation phase being shortened as the curing temperature is increased. The second effect shows, for instance, that mortar cured at 50°C shows a loss of attainable strength of 23%, compared with that cured at 12.5°C. This demonstrates the necessity of accounting for the effect of the temperature in a realistic chemoaging model, particularly for higher curing temperatures.

The overall agreement between experimental and numerical results is very good. Both significant effects of the curing temperature in the evolution of the strength are well captured with the present model. Note that the proposed model allows for remarkably good predictions for curing temperatures below and above the reference temperature.

Wild et al. Tests

The second set consists of tests conducted by Wild et al. (1995). The results used here refer to ordinary portland concrete, the mix being designed according to the U.S. Department of the Environment specifications with the aim of producing high-strength concrete (70 MPa). The material properties used for the numerical simulation are listed in Table 1.

Fig. 4 shows the compressive strength versus time curves obtained for the curing temperatures T_0 = 20 and 50°C, respectively. The dots represent the experimental values, the solid line is the prediction by the model, and the dashed line is the result obtained by neglecting the influence of the temperature in the evolution of the aging function. Note that concrete cured at 50°C shows a loss of attainable strength of 6%, compared with that cured at 20°C, which is significantly less than the percentage measured for the mortar tested by Kjellsen. The overall agreement obtained between numerical and experimental results is good.

CONCLUSIONS

This paper describes a thermo-chemo-mechanical model that accounts for many of the features observed in the behavior of concrete at early ages. An appropriate thermodynamic framework is provided for these irreversible processes. Expressions for the free energy are provided from which the state equations are derived. Positive dissipation is guaranteed in all situations. The hydration model is based on the reactive porous media theory on its thermochemical part. A novel aging model

J. Eng. Mech., 1999, 125(9): 1018-1027

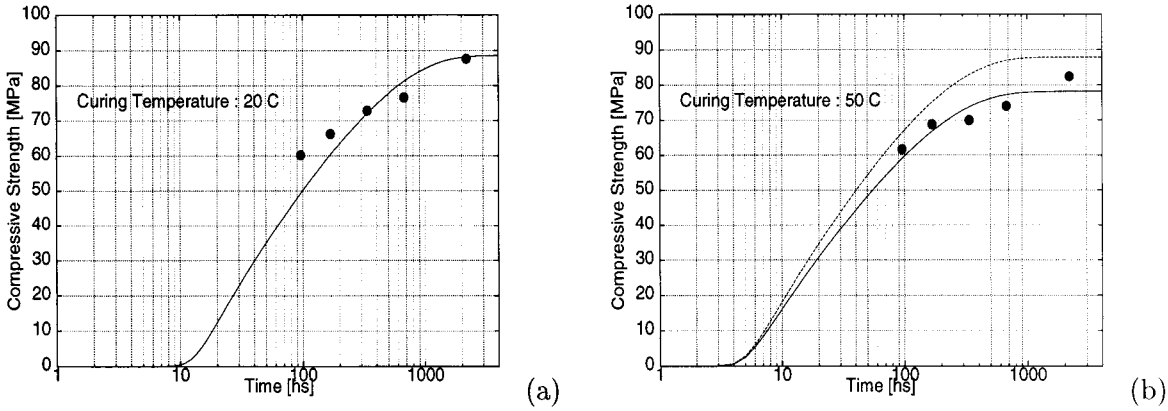

FIG. 4. Strength Evolution for Wild et al. Tests

is introduced that accounts for the effect of the curing temperature in the evolution of the relevant mechanical properties. The aging degree is introduced as an internal variable, different from the commonly used hydration degree or maturity concepts. The model is well suited for its implementation in a finite-element program devised for thermal analysis. The capabilities and potentiality of the model are shown by performing numerical simulations of adiabatic and isothermal tests in concrete samples. The qualitative and quantitative agreement between the model results and the available experimental data is remarkably good in all situations.

APPENDIX I. REFERENCES

Acker, P. (1988). ''Comportement mecanique du beton: Apports de l'aproche physico-chimique.'' *Raport de recherche N. 152*, Laboratoire Ponts et Chaussées, Paris (in French).

Acker, P. (1997). ''Dispositif d'étude de la cinétique d'hydratation des bétons par calimétrie isotherme.'' *Bull. liaison Laboratoire Ponts et Chaussées*, Paris, 210, 31–40.

Bentz, D. P., Waller, V., and de Larrard, F. (1998). ''Prediction of adiabatic temperature rise in conventional and high-performance concretes using a 3-d microstructural model.'' *Cement and Concrete Res.*, 28(2), 285–297.

Bland, C., Poole, A., and Patel, H. (1994). ''The microstructure of concrete cured at elevated temperatures.'' *Proc., Inst. of Mat. Conf. on Cement and Concrete Sci.*

Boumiz, A., Vernet, C., and Tenoudji, F. C. (1996). ''Mechanical properties of cement pastes and mortars at early ages.'' *Adv. Cem. Bas. Mat.*, 3, 94–106.

Byfors, J. (1980). ''Plain concrete at early ages.'' *Tech. Rep. No. 3:80*, Swedish Cement and Concrete Research Institute, Stockholm.

Carino, N. J. (1981). ''Temperature effects on the strength-maturity relation of mortar.'' *Tech. Rep. No. NBSSIR 81-2244*, National Bureau of Standards, Washington, D.C.

CEB-FIP model code 1990. (1990). Comité Euro-International du Beton.

Chengju, G. (1989). ''Maturity of concrete method for predicting early-stage strength.'' *ACI Mat. J.*, 86(4), 341–353.

Copeland, L. E., Kantro, D. L., and Verbeck, G. (1960). ''Chemistry of hydration of cement.'' *Proc. 4th Int. Symp., Chemistry of Cement*, Paper IV-3.

Coussy, O. (1995). *Mechanics of porous media.* Wiley, New York.

de Schutter, G., and Taerwe, L. (1995). ''General hydration model for portland cement and blast furnace slag cement.'' *Cement and Concrete Res.*, 25(3), 593–604.

de Schutter, G., and Taerwe, L. (1996). ''Degree of hydration based description of mechanical properties of early age concrete.'' *Mat. and Struct.*, Paris, 29, 335–344.

de Schutter, G., and Taerwe, L. (1997). ''Fracture energy of concrete at early ages.'' *Mat. and Struct.*, Paris, 30, 67–71.

Hansen, P. F., and Nielsen, A. (1985). ''Method for quick calculation of temperature differences in concrete members.'' *Proc., VTT Symp. 61.*

Instrucción para el proyecto y la ejecución de obras de hormigón en masa o armado. (1991). MOPT (in Spanish).

Kim, J.-K., Moon, Y.-H., and Eo, S.-H. (1998). ''Compressive strength development of concrete with different curing time and temperature.'' *Cement and Concrete Res.*, 28(12), 1761–1773.

Kjellsen, K. O. (1990). ''Physical and mathematical modeling of hydration and hardening of portland cement concrete as a function of time and curing temperature,'' PhD thesis, Div. of Build. Mat., Norwegian Institute of Technology.

Kjellsen, K. O., and Detwiler, R. J. (1993). ''Later-age strength prediction by a modified maturity model.'' *ACI Mat. J.*, 90(3), 220–227.

Mak, S. L., and Torri, K. (1995). ''Strength development of high strength concretes with and without silica fume under the influence of high hydration temperatures.'' *Cement and Concrete Res.*, 25(8), 1791–1802.

''Mass concrete.'' (1987). *ACI manual of concrete practice, ACI 207.1R-87*, American Concrete Institute.

Neville, A. M. (1981). *Properties of concrete.* Wiley, New York.

Oloukon, F. A., Bourdette, E. G., and Deatherage, J. H. (1990). ''Early-age concrete strength prediction by maturity—another look.'' *ACI Mat. J.*, 87(6), 565–572.

Pantazopoulo, S. J., and Mills, R. H. (1995). ''Microstructural aspects of the mechanical response of plain concrete.'' *ACI Mat. J.*, 92(6), 605–616.

Parrot, L., Geiker, M., Gutteridge, W., and Killoh, D. (1990). ''Monitoring portland cement hydration: Comparison of methods.'' *Cement and Concrete Res.*, 20(6), 919–926.

Plowman, J. M. (1956). ''Maturity and strength of concrete.'' *Mag. of Concrete Res.*, 8(22), 13–22.

Rastrup, E. (1954). ''Heat of hydration in concrete.'' *Mag. of Concrete Res.*, 6(17), 2–13.

Reinhardt, H. W., Blaauwendraad, J., and Jongedijk, J. (1982). ''Temperature development in concrete structures taking account of state dependent properties.'' *Proc., Int. Conf. of Concrete at Early Ages.*

Rostassy, F. S., Gustsch, A., and Laube, M. (1993). ''Creep and relaxation of concrete at early ages—Experiments and mathematical modelling.'' *Proc., 5th Int. RILEM Symp. on. Creep and Shrinkage of Concrete*, H. Mang, N. Bicanic, and R. de Borst, eds., E & FN Spon, London.

Saul, A. G. A. (1951). ''Principles underlying the steam curing of concrete at atmospheric pressure.'' *Mag. of Concrete Res.*, 2(6), 127–140.

Shi, C., and Day, R. L. (1993). ''Acceleration of strength gain of lime-pozzolan cements by thermal activation.'' *Cement and Concrete Res.*, 23(4), 824–832.

Tan, K., and Gjorv, O. E. (1996). ''Performance of concrete under different curing conditions.'' *Cement and Concrete Res.*, 26(3), 355–361.

Torrenti, J. M. (1992). ''La résistance du béton au trés jeunge age (in French).'' *Bull. liaison Laboratoire Ponts et Chaussées*, 179, 31–41.

Torrenti, J. M., Guénot, I., Laplante, P., Acker, P., and Larrand, F. (1994). ''Numerical simulation of temperatures and stresses in concrete at early ages.'' *Proc., Int. Conf. on Computational Modelling of Concrete Struct.*, Z. P. Bazant and I. Carol, eds., Pineridge, Swansea, U.K., 559–568.

Ulm, F. J., and Coussy, O. (1995). ''Modeling of thermochemomechanical couplings of concrete at early ages.'' *J. Engrg. Mech.*, ASCE, 121(7), 785–794.

Ulm, F. J., and Coussy, O. (1996). ''Strength growth as chemo-plastic hardening in early age concrete.'' *J. Engrg. Mech.*, ASCE, 122(12), 1123–1132.

van Breugel, K. (1992a). ''Hysmostruc: A computer based simulation model for hydration and formation of structure in cement based materials.'' *Hydration and setting of cements*, A. Nonat and J. C. Mutin, eds., RILEM, Essen, Germany, 361–368.

van Breugel, K. (1992b). ''Numerical simulation and microstructural development in hardening cement-based materials.'' *Heron*, 37(3), 1–61.

Verbeck, G. J., and Helmuth, R. H. (1968). ''Structures and physical

properties of cement paste.'' *Proc., 5th Int. Symp. on the Chem. of Cement*, 1–32.
Volz, C. K., Tucker, R. L., Burns, N. H., and Lew, H. S. (1981). ''Maturity effects on concrete strength.'' *Cement and Concrete Res.*, 11(1), 41–50.
Walker, S., and Bloem, D. L. (1958). ''Variations in portland cement.'' *Proc., ASTM, 58*, 1009–1032.
Walker, V., de Larrard, F., and Roussel, P. (1996). ''Utilization of high-strength/high-performance concrete.'' *Proc., 4th Int. Symp. RILEM*, RILEM, Essen, Germany, 415–421.
Wild, S., Sabir, B. B., and Khatib, J. M. (1995). ''Factor influencing strength development of concrete containing silica fume.'' *Cement and Concrete Res.*, 25(7), 1567–1580.

APPENDIX II. NOTATION

The following symbols are used in this paper:

A_f, B_f = material properties for aging evolution;
$\tilde{A}_\xi$ = normalized chemical affinity;
A_ξ, $A_{\xi 0}$ = chemical affinity, initial chemical affinity (ref. to ξ);
A_χ, $A_{\chi 0}$ = chemical affinity, initial chemical affinity (ref. to χ);
C = heat capacity per unit volume;
$\mathcal{D}$, $\mathcal{D}_{chem}$ = dissipation, chemical dissipation;
E, E_∞ = elastic modulus, final elastic modulus;
E_a = activation energy;
$f^\pm$, $f^\pm_\infty$ = tensile compressive strength, final values;
$f^\pm_e$ = elastic limit in uniaxial tests (tension/compression);
f^-_{set} = compressive strength at setting;
$G^\pm_f$ = tensile/compressive fracture energy;
H = chemical contribution to free energy;
K, G = bulk and shear moduli;
k_T = thermal conductivity;
L = thermomechanical contribution to free energy;
n_T = exponent for strength evolution;
R = constant for ideal gases;
R_{ext} = external volume heat sources;
Q = hydration heat per unit volume;
$\mathbf{Q}$ = heat flux;
Q_χ, Q_ξ = hydration heat per unit of hydration extent, (°);
Q_∞ = final amount of liberated heat (in ideal conditions);
S = entropy;
s/c = silica fume/cement mass ratio;
T, T_0 = temperature, initial temperature;
T^{ad}_∞, $\bar{T}^{ad}_\infty$ = final reached temperature in adiabatic test, as in ideal conditions;
T^{iso} = temperature for curing in isothermal conditions;
T_{ref} = reference temperature;
T_T = maximum temperature for strength evolution;
V = thermal contribution to free energy;
w/c = water/cement mass ratio;
$\bar{\eta}$ = exponent for viscosity;
η_ξ, $\eta_{\xi 0}$ = viscosity, reference viscosity (ref. to ξ);
η_χ, $\eta_{\chi 0}$ = viscosity, reference viscosity (ref. to χ);
κ = aging degree;
κ_∞, κ^{iso}_∞ = final aging degree, as in isothermal conditions;
λ_E = elastic modulus aging function;
$\lambda^\pm_f$ = tensile/compressive strength aging function;
$\lambda^\pm_G$ = tensile/compressive fracture energy aging functions;
μ_t = maturity;
ν = Poisson's ratio;
ξ, ξ_{set} = hydration degree, hydration degree at setting;
ξ_∞, $\bar{\xi}_\infty$ = final hydration degree, as in ideal conditions;
χ = hydration extent;
χ_∞, $\bar{\chi}_\infty$ = final hydration extent, as in ideal conditions; and
Ψ = free energy.